Interaction Notes

Note 353

September 29, 1978

THE RECEIVING PROPERTIES OF THE SMALL ANNULAR SLOT ANTENNA

David E. Merewether, Roger B. Cook and Robert Fisher

ELECTRO MAGNETIC APPLICATIONS, INC.
P. O. Box 8482
Albuquerque, New Mexico 87198

Abstract

An analytical formula for the effective height of an annular slot antenna is determined using the reciprocity theorem. This result generalizes the previously available monochromatic result and yields an equivalent cirucit valid for computing the transient response of the small annular slot antenna.

THE RECEIVING PROPERTIES OF THE SMALL ANNULAR SLOT ANTENNA

1. INTRODUCTION

The annular slot antenna (Figure 1) has been a subject of continuing interest because it is a low profile antenna [1] and because it is a tractable model for the inadvertant antenna formed by the recessed connectors used on some missiles [2]. The problem of predicting the receiving properties of this antenna is complicated by the fact that the field distribution in the aperture is not strictly TEM (ie., $E_r \sim \frac{1}{r}$). Although the exact distribution of the field in the aperture is not required for predicting the radiated field, the contribution of higher order TM modes to the equivalent antennna capacity is not negligible [3].

The problem can be circumvented by locating the drive terminals at a distance below the ground plane where the TM modes have all disappeared. An apparent antenna admittance and an apparent effective height referred to the ground plane is calculated in this way. This approach was used by Chang and Harrison to find the effective height of an annular slot as observed across a conjugate matched load located one helf of a wavelength from the opening [4]. While their results may have been suitable for continuous wave

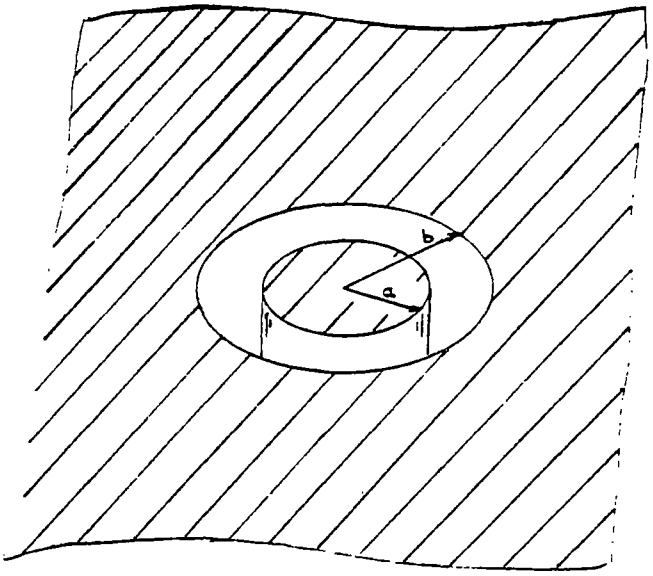

Figure 1. Annular Slot Antenna

analysis, for pulse response analysis a less restrictive result is required. In their own work, Chang and Harrison used a formula for the short circuit current ([5] eq. 23),

$$I_o = -j4\pi a E_o \xi_o^{-1} J_1(k_o a \sin\theta_o) \tag{1}$$

where common definitions are used, $k_o = \omega/c$, $\xi_o = \sqrt{\frac{\mu_o}{\varepsilon_o}}$, etc. This result was expected to be true for the thin slot with $(b-a) << b$.

Evidently, in (1) E_o is the incident field at the observer location without the ground plane or the antenna present. For most problems the ground plane would exist with or without the antenna present. For these problems a more natural incident field is the normal component of the total electric field observed at the antenna location without the antenna present,

$$E^{norm} = 2 E_o \sin\theta_o. \tag{2}$$

Noting that for small arguments $J_1(x) = \frac{x}{2}$ (1) becomes

$$I_o(\omega) = -j4\pi a \frac{E^{norm}}{2 \sin\theta_o} \xi_o^{-1} \frac{k_o a \sin\theta_o}{2} \tag{3}$$

$$= -j\omega\varepsilon_o E_{norm} \pi a^2. \tag{4}$$

So that

$$I_o(t) = -\text{Area } \varepsilon_o \frac{dE^{norm}}{dt} \tag{5}$$

which is the result expected by physical intuition. In the EMP handbook [2] the data was normalized to E_o and this formula was used for small values of a/b.

Here, we derive a new formula for the effective height, based on the reciprocity theorem that is valid for pulse analysis and is not restricted to very thin slots.

Following this development, the formula for antenna capacity is examined to determine its limitations. Parametrically determined data is given to provide a complete description of the equivalent circuit for a range of a/b values from 0.3 to 1.

In the final section, a finite difference approach was used to obtain supporting data for the new effective height formulas.

2. DERIVATION OF EFFECTIVE HEIGHT FORMULA

Consider the annular slot antenna driven by a continuous wave current source I_1, located some distance below the exit plane (Figure 2). Consider that a small current element $I_2(2h_2)$ is simultaneously radiating at the same frequency and that its direction is along the hemisphere centered on the antenna. Then, according to the reciprocity theorem ([6], p. 322), we may expect that

$$\int_v \vec{E}_2 \cdot \vec{J}_1 \, dv = \int_v \vec{E}_1 \cdot \vec{J}_2 \, dv \tag{6}$$

Here, E_1 and E_z are the electric fields produced by the distributed currents source density $\vec{J}_1$, and $\vec{J}_z$ respectively and the volume integral includes both sources. Since the current source $\vec{J}_1$ exists only at the load inside the coax $\vec{J}_1 = I_1 (2\pi r)^{-1} \vec{a}_r \, \delta(z+d)$, and the left side of (6) is

$$\int_v \vec{E}_2 \cdot \vec{J}_1 \, dv = I_1 \int_a^b E_{2r} \, dr \tag{7}$$

$$= I_1 * (\text{Voltage across load due to source \#2})$$

Assuming that this voltage is induced at the end of the coax, then

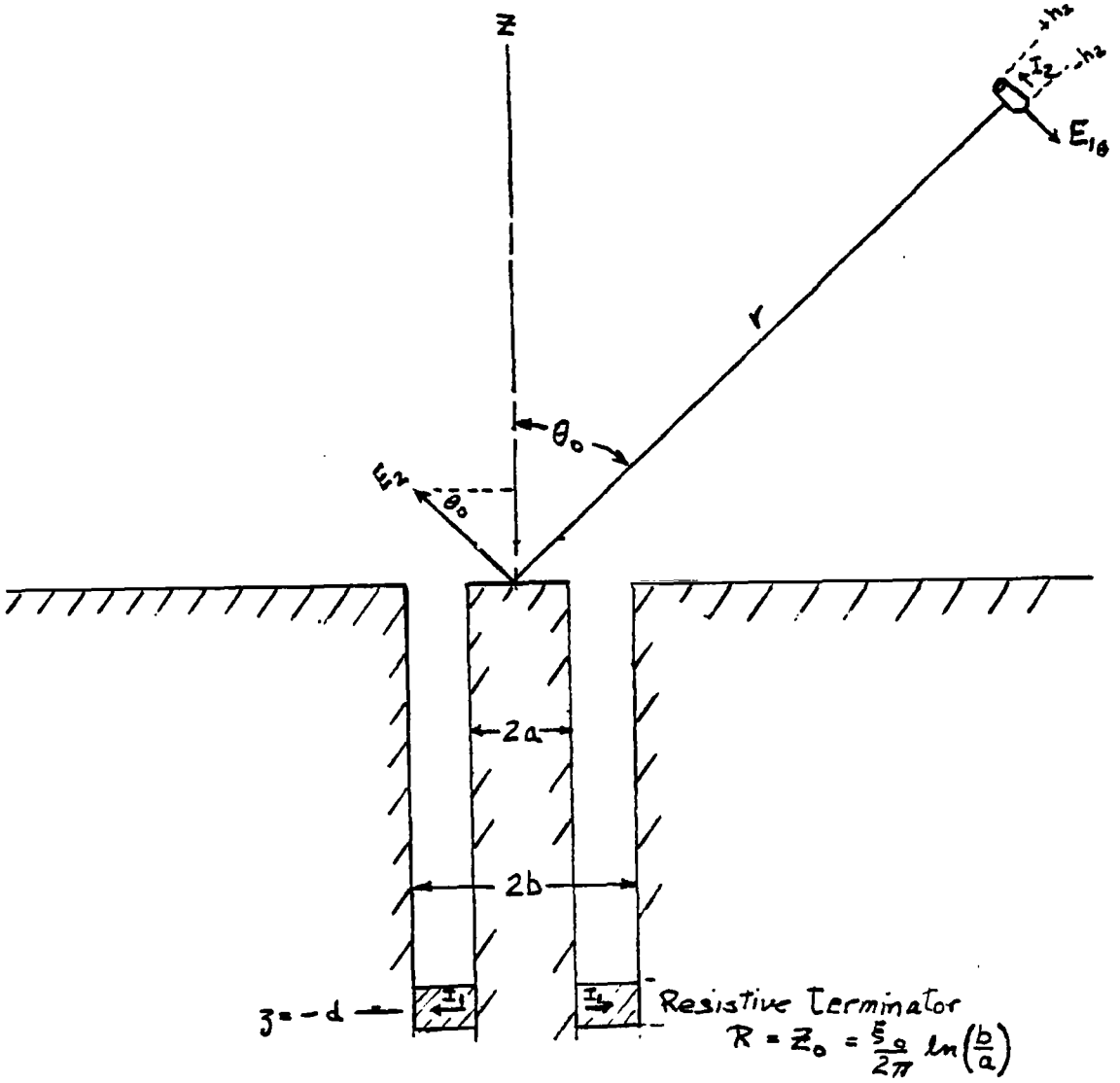

Figure 2: Driven Annular Slot Antenna with Test Source

$$\int_v \vec{E}_2 \cdot \vec{J}_1 \, dr = I_1 * h_e \, E_2^{norm} * \frac{Z_o}{Z_a + Z_o} \, e^{-jk_o d} \, . \qquad (8)$$

Here, Z_a is the effective antenna impedance and Z_o is the characteristic impedance of the transmission line and E_2^{norm} is the normal component of the incident field due to the test source ([6], p. 310) and its image at the top of the annular slot.

$$E^{norm} = -j \frac{\omega\mu 2 * I_2 * 2h_2}{4\pi r} e^{-jk_o r} \sin\theta_o \qquad (9)$$

Finally, the left side of (6) is

$$\int_v \vec{E}_2 \cdot \vec{J}_1 \, dv = \frac{-I_1 h_e Z_o}{Z_a + Z_o} * e^{-jk_o(r+d)} \frac{j\omega\mu I_2 \, h_2 \sin\theta_o}{\pi r} \qquad (10)$$

The right side of equation 6 is evaluated by noting that the test source is oriented along the $-\vec{a}_\theta$ direction so that only the E_θ component of $\vec{E}_1$ is important:

$$\int_v \vec{E}_1 \cdot \vec{J}_2 \, dv = I_2 \int_{-h_2}^{h_2} E_1 \cdot -(\vec{a}_\theta) dz' = - I_2 \, 2h_2 \, E_{1\theta} \, . \qquad (11)$$

$E_{1\theta}$ has been determined by Harrison and Chang [4, Eq. 24].

$$E_{1\theta} \doteq - \frac{V_a e^{-jk_o r}}{r \, \ell n \, b/a} \left[J_o(k_o b \sin\theta_o) - J_o(k_o a \sin\theta_o) \right], \qquad (12)$$

which is computed assuming that E_{1r} is TEM at the aperture:

$$E_{1r} = \frac{V_a}{\rho \, \ell n(b/a)} \, . \qquad (13)$$

Now if the aperture voltage V_a is due to a source, J_1 at $z = -d$, we have

$$V_a = \frac{I_1 Z_o Z_a}{Z_o + Z_a} e^{-jk_o d} \tag{14}$$

Using (11), (12) and (14), the right side of equation (6) becomes

$$\int_v \vec{E}_1 \cdot \vec{J}_2 \, dv = \frac{+I_2 2h_2 \, e^{-jk_o(r+d)}}{r \, \ell n \, b/a} \left[J_o(k_o b \sin \theta_o) - J_o(k_o a \sin \theta_o) \right] \frac{I_1 Z_o Z_a}{Z_o + Z_a} \tag{15}$$

Substituting (10) and (15) into (6), the effective height is determined to be

$$h_e = \frac{-2\pi Z_a \left[J_o(k_o b \sin \theta_o) - J_o(k_o a \sin \theta_o) \right]}{j\omega\mu \, \ell n \, (b/a) \sin \theta_o} . \tag{16}$$

If the antenna is small, $k_o b < 1$, then $Z_a \simeq \frac{1}{j\omega C_a}$ and $J_o(X) \simeq 1 - \frac{X^2}{4}$ such that

$$h_e = \frac{\pi\varepsilon(b^2 - a^2)}{2 C_a \, \ell n(b/a)} \sin \theta_o . \tag{17}$$

The form of (16) is similar to the monochromatic result given by Harrison and Chang ([4]eq. 61). However, the assumptions used here are less restrictive so that the effective height given by (16) is valid for computing the voltage measured across any impedance at a reasonable distance ($d > 5b$) below a ground plane using transmission line theory. Equation (17) is suitable for pulse response studies provided that $k_o b < 1$ at the highest frequency of interest.

3. EQUIVALENT CIRCUIT FOR AN ANNULAR SLOT ANTENNA

The voltage or current equivalent circuit of an annular slot antenna is useful for determining the electromagnetic energy that is coupled into cables with arbitrary loads on the far end. This section presents the frequency domain formulation of the equivalent circuits, with the inherent assumptions that only TEM modes exist. The time domain formulation, including TEM and TM modes, is derived in Section 4 of this report.

The equivalent circuits consist of a current (or voltage) source in parallel (or series) with the aperture capacitance as shown in Figure 3. Both time and frequency domain sources are shown.

The aperture admittance was derived by Levine and Papas [7], and is given by the following equation:

$$Y_a = G_a + j\omega C_a \tag{18}$$

with

$$G_a = \frac{Y_o}{\ell n\ b/a} \int_o^{\pi/2} \frac{d\theta}{\sin\theta} \left[J_o(k_o a \sin\theta) - J_o(k_o b \sin\theta) \right]^2 \tag{19}$$

$$\omega C_a = \frac{Y_o}{\pi \ell n\ b/a} \left[2 \int_o^{\pi} d\psi\ S_i \left\{ k_o a \left[1 + (b/a)^2 - 2\ (b/a) \cos\psi \right]^{\frac{1}{2}} \right\} \right.$$

$$\left. - \int_o^{\pi} d\psi\ S_i(2k_o a \sin\frac{\psi}{2}) - \int_o^{\pi} d\psi\ S_i\ (2k_o b \sin\frac{\psi}{2}) \right] \tag{20}$$

with S_i representing the sine integral, and $Y_o = \frac{1}{60\ \ell n\ b/a}$, the characteristic admittance of the cable. For EMP and lightning calculations, and for typical annular slot antenna geometries, the small argument expansion ($k_o b \ll 1$) is valid, and these equations reduce to the following:

$$G_a = \frac{2Y_o}{3\ell n\ b/a}\left(\frac{k_o a}{2}\right)^4 \left[(b/a)^2 - 1\right]^2 \qquad (21)$$

and

$$\omega C_a = \frac{2k_o a\ Y_o}{\pi \ell n\ b/a}\left(\int_o^{\pi} d\psi \left[1 + (b/a)^2 - 2(b/a)\cos\psi\right]^{\frac{1}{2}} - 2\ (1 + b/a)\right). \qquad (22)$$

The conductance G_a is frequency dependent, and can not be represented in a time domain circuit; however, G_a is small and can usually be neglected except when the load connected to the equivalent circuit is a very high impedance.

The normalized C_a, calculated from (22) is shown in Figure 3, along with the normalized h_e obtained from (17).

Since the antenna capacity is very small, the current equivalent circuit would be appropriate for most problems involving cables terminated in realistic impedances. The product $C_{ant}\ h_e$ needed for this equivalent is also given on Figure 3.

The effect of recessing the center post of the antenna was not considered in this work. The depth dependence shown on Figure 3 was taken from Reference 2.

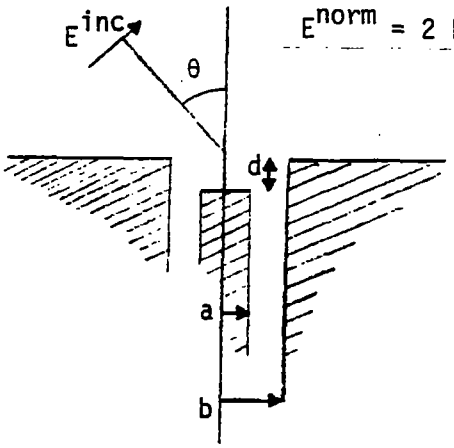

$E^{norm} = 2\,E^{inc} \sin\theta$

Antenna Configuration

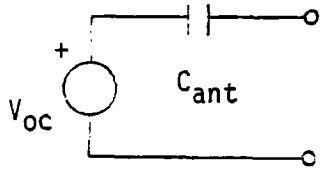

$V_{oc} = h_e E^{norm}(t)$, or
$V_{oc} = h_e E^{norm}(\omega)$

Voltage Equivalent Circuit

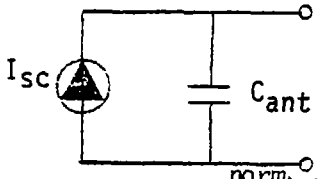

$I_{sc} = C_{ant} h_e \frac{\partial E^{norm}(t)}{\partial t}$, or

$I_{sc} = j\omega C_{ant} h_e E^{norm}(\omega)$

Current Equivalent Circuit

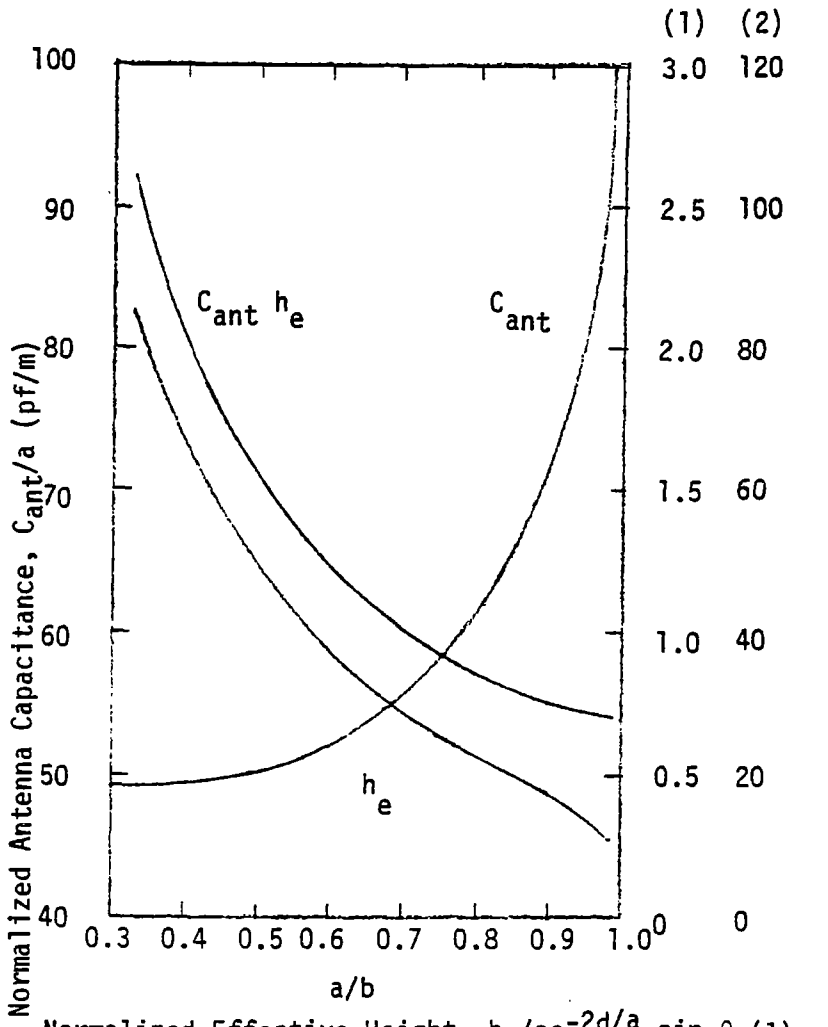

Figure 3: The Equivalent Circuits

4. FINITE DIFFERENCE PREDICTIONS OF EQUIVALENT CIRCUIT PARAMETERS

All of the analytical results given in Sections 2 and 3 are based on the approximation that the fields within the coaxial region are TEM, and consequently, one can question the accuracy of these results, particularly for small ratios of a to b. As a qualitative check on the adequacy of the TEM approximations, numerical predictions of the antenna capacity and effective height were made using the finite difference technique [8].

Effective antenna height and antenna capacitance were evaluated from the numerical data produced by the code. The geometry used in this code is summarized in Figure 4. The antenna was driven by a unit amplitude current source of gaussian form with a matched load at the base of the antenna. The source current is split between the resistive load and the antenna, hence the peak current on the center conductor was .5 amp. A far field radiation boundary condition [8] was employed at a height of five times the slot radius and at ten times the slot radius in the radial direction. The antenna drive point was at the bottom of the antenna coax region five slot radii in depth from the aperture. The various boundaries were maintained constant while the antenna radius was varied. The values of the ratio of the antenna radius to the slot outer radius that were studied were a/b = .95, .9, .7, .5, .3, and .1.

In order to evaluate the effective antenna height and the capacitance from the finite difference data, it is necessary to relate these parameters to the fields predicted by the computer code. We will develop here the relationships providing these parameters. Consider first the antenna capacitance. This capacitance is given by

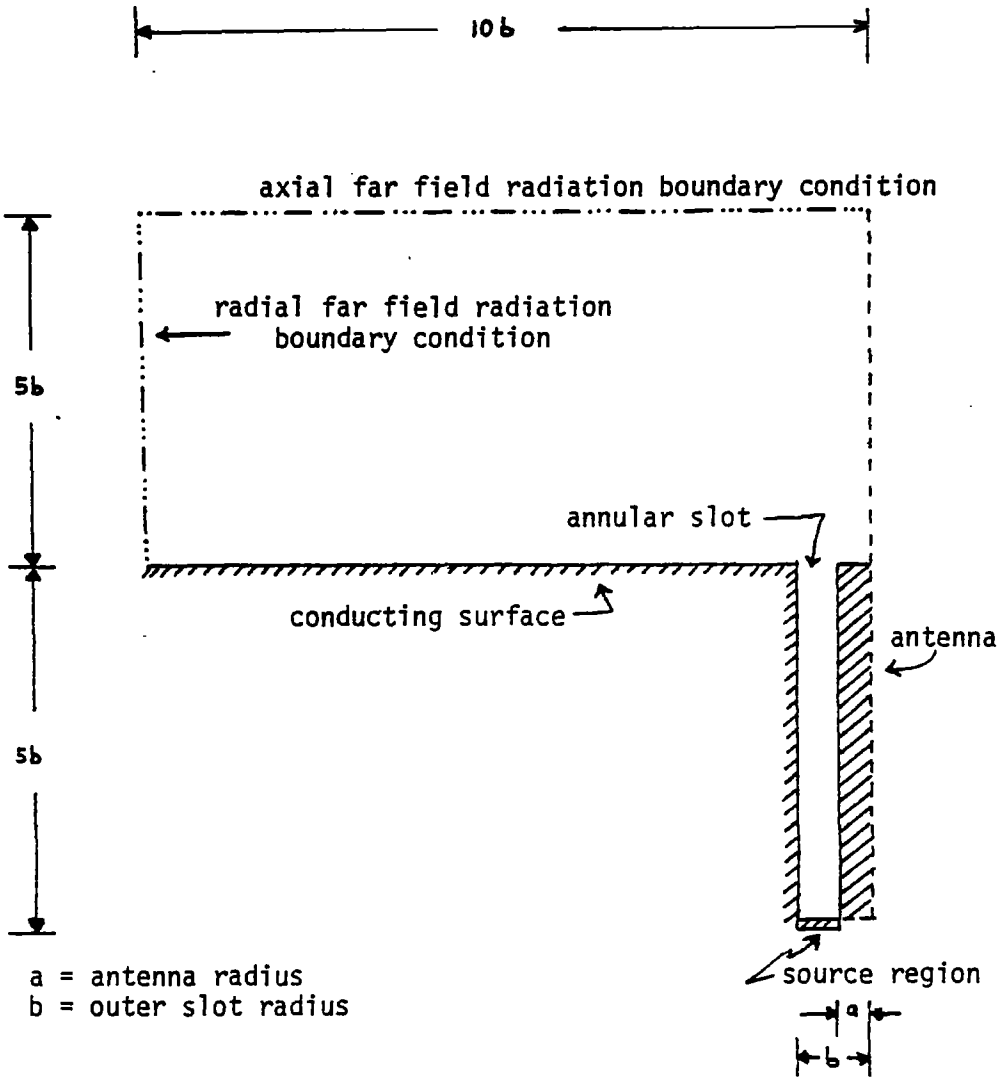

Figure 4: Geometry for finite difference computations

$$C_a = \frac{Q}{V_a} , \tag{23}$$

where V_a is the antenna aperture voltage and Q is the charge developed at the aperture. However, the charge term can be rewritten as

$$Q = \int I \, dt = \frac{\int (V_c - V_a) \, dt}{Z_o} \tag{24}$$

V_c is the TEM voltage that would occur if the coaxial cable were open circuited and Z_o is the characteristic impedance of the slot. Evidently, the antenna capacitance should be given by,

$$C_a = \frac{\int (V_c - V_a) \, dt}{V_a \, Z_o} . \tag{25}$$

To facilitate this computation, the aperture fields were integrated to compute the coaxial and aperture voltages required to perform the integration in (25). The results of these computations are compared with the analytical results in Section 5.

The antenna effective height can also be determined from the time domain computer code. Since the higher order TM modes are included in this calculation, it is possible to calculate an approximate value for the effective height without the TEM assumption. As in Section 2, we position a TEM exciting source far enough away from the groundplane that the TEM assumption can be expected to be valid for both the transmitted and received fields. We return to (6) and define a new effective height h_{eZ_o} such that $h_{eZ_o} \; E^{inc}$ = the voltage across a resistor equal to the characteristic impedance of the coaxial cable. With this assumption (10) becomes

$$\int E_2 \, I_1 \, dr = I_1 \, h_{eZ_o} \left(\frac{j\omega\mu_o \, I_2 \, 2h_2}{4\pi r} \right) e^{-jk_o(r+d)} , \tag{26}$$

where the test source is a monopole of height h_2 located on the ground plane $\theta_o = \pi/2$ (Figure 2). For the right side of equation (6), we are to use the numerically predicted radiated field at the point r, then (15) becomes

$$\int E_i \cdot I_2 \, dv = E_{z1}(r) \, I_2 \, h_2 \, , \tag{27}$$

and applying (6), we have

$$h_{eZ_o} = \frac{2\pi r \, E_{z1}(r)}{j\omega\mu_o \, I_1 e^{-jk_o(r+d)}} \, . \tag{28}$$

The results of these calculations can be related to the open circuit effective height by substitution into the equivalent circuit of Figure 3.

$$\frac{h_e E^{norm} * Z_o e^{-jk_o d}}{Z_a + Z_o} = h_{eZ_o} \, E^{norm} . \tag{29}$$

Recognizing that $Z_a = \frac{1}{j\omega C_a} >> Z_o$,

$$h_e \doteq h_{eZ_o} \, \frac{Z_a}{Z_o} \, e^{-jk_o d} \doteq \frac{2\pi r \, E_{z1}(r)}{\mu_o \, C_a \, Z_o \, (j\omega)^2 \, I_1} \, . \tag{30}$$

The results of the computer predictions made using a Gaussion input pulse showed that $E_{z1}(r)$ was similar in shape to the second derivative of $I_1(t)$ (Figure 5). However, the pulse that was used as an input was too short to satisfy the requirement that $k_o b << 1$ at every frequency. As a result, Fourier transforms of the field predictions were substituted into (30) to obtain the results given in Section 5.

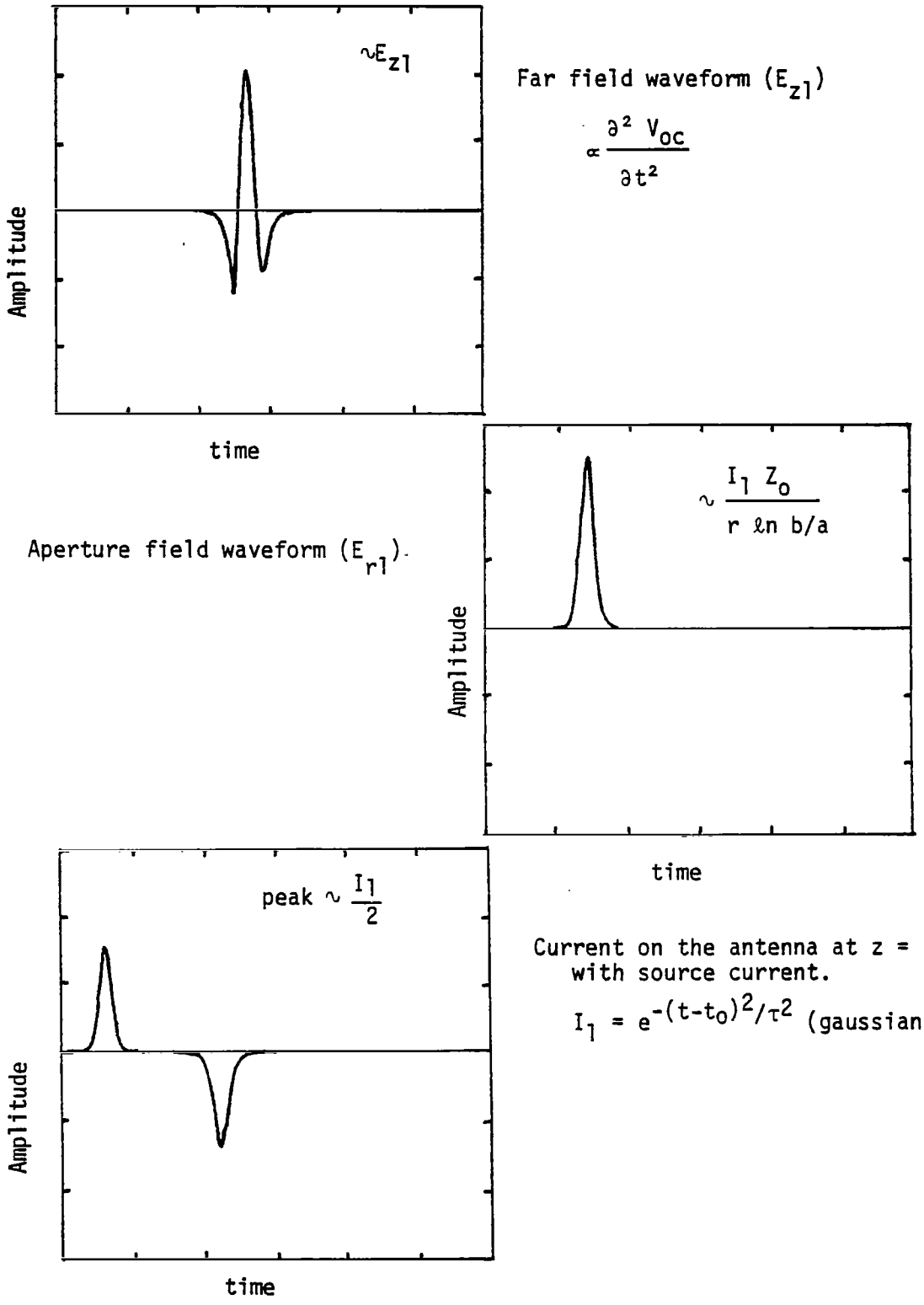

Figure 5: Typical waveforms from the finite difference code

5. COMPARISON OF RESULTS AND CONCLUSIONS

The two solution approaches used here both are based on the reciprocity theorem. However, the analytical results for both effective height and antenna capacity assume that only TEM fields exist in the coaxial cable, while the finite difference approach approximately accounts for all TM modes. The accuracy of the finite difference calculations improves as the slot width increases, since there are more finite difference cells in the aperture, while the accuracy of the analytical result should decrease as the slot width increases.

The results of the two prediction techniques are compared in Figure 6. The antenna capacity for this type of antenna is very small, so it was expected to be difficult to extract from the finite difference results. However, the disagreement between the two predictions of antenna capacity was less than 25% over the entire range of a/b. The calculations of the effective height and the short circuit current disagree by less than 10%. We conclude, therefore, that the most serious inaccuracies are in the computation of the antenna capacity.

In any event, the comparisons suggest that the analytical formulas given in Sections 2 and 3 (or shown in Figure 3) are sufficiently accurate to use for EM susceptibility analysis across the range of $.3 < a/b < .9$.

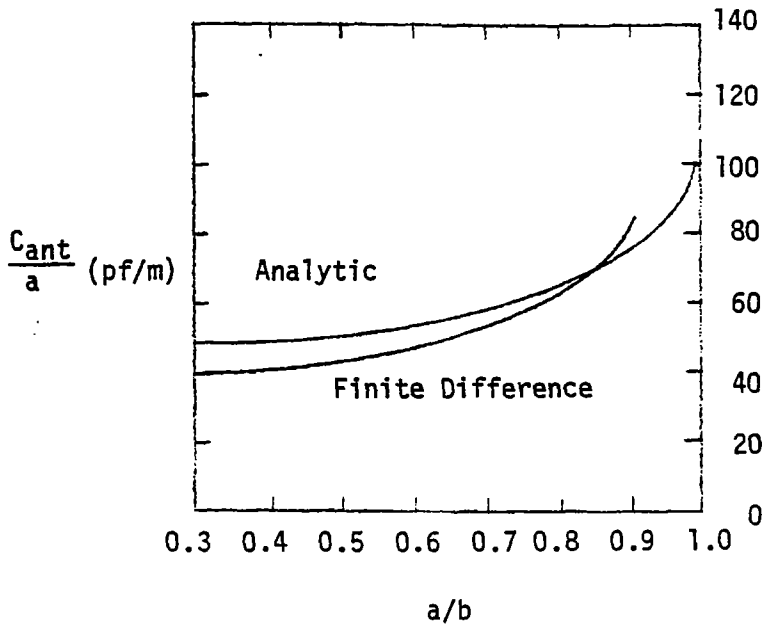

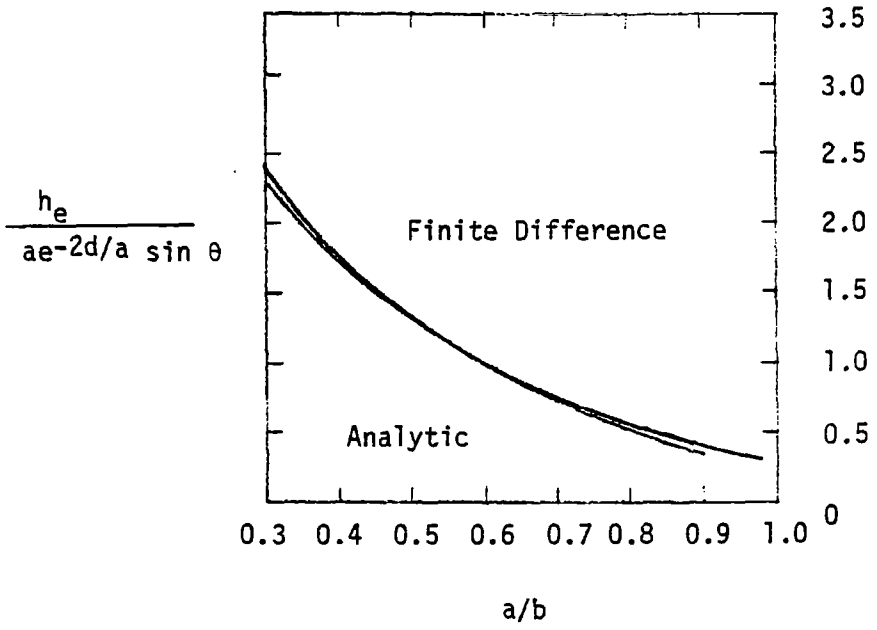

Figure 6: Comparison of Frequency and Time Domain Results

REFERENCES

1. Jones, J. E. and Richmond, J. H., "Application of an Integral Equation Formulation to the Prediction of Space Shuttle Annular Slot Antenna Radiation Patterns," IEEE Trans. on Antennas and Propagation, Vol. AP 22, No. 1, January 1974, pp 109-111.

2. Sandia Labs, "Electromagnetic Pulse Handbook for Missiles and Aircraft in Flight", Air Force Weapons Lab, EMP Interaction 1-1, September 1972.

3. Chang, D. C. "Input Impedance and Complete Near Field Distribution of an Annular Aperture Antenna Driven by a Coaxial Line," IEEE Transactions on Antennas and Propagation, Vol. AP-18, No. 5, September 1970, pp 610-616.

4. Harrison, C. W. and D. C. Chang, "Theory of the Annular Slot Antenna Based on Duality," IEEE Transactions on EMC, Vol. EMC-13, No. 1, February 1971, pp 8-14.

5. Chang, D. C. and C. W. Harrison, "On the Pulse Response of a Flush Mounted Coaxial Aperture", IEEE Transactions on EMC, Vol. EMC-13, No. 1, February 1971, pp 14-18.

6. Weeks, W. L. Electromagnetic Theory for Engineering Applications, John Wiley and Sons, Inc., New York, 1964.

7. Levine, H. and Papas, C. H., "Theory of the Circular Diffraction Antenna", Journal of Applied Physics, Vol. 22, Jan. 1951, pp 29-43.

8. Merewether, D. E., "Transient Currents Induced on a Body of Revolution by an Electromagnetic Pulse", IEEE Transactions on EMC, Vol. EMC-13, No. 2, May 1971, pp 41-46, and also Interaction Note 93, May 1971.